

Surface Modification of Mesoporous Nanosilica with [3-(2-Aminoethylamino) propyl] trimethoxysilane and Its Application in Drug Delivery

Z. Mohamadnia¹, E. Ahmadi², M. Ghasemnejad², S. Hashemikia³ and A. Doustgani^{2,4}

1. Department of chemistry, Institute for Advanced Studies in Basic Sciences (IASBS), Gava zang, Zanjan, I. R. Iran.

2. Department of chemistry, University of Zanjan, Zanjan, I. R. Iran.

3. Department of Textile Engineering, Center of Excellence in Textile, Amirkabir University of Technology (Tehran Polytechnic), Tehran, I. R. Iran.

4. Department of Chemical Engineering, University of Zanjan, Zanjan, I. R. Iran.

(*) Corresponding author: z.mohamadnia@iasbs.ac.ir
(Received: 13 April 2015 and Accepted: 11 Sep. 2015)

Abstract

Mesoporous silica nanoparticles with unique structure (SBA-15) were synthesized and modified by [3-(2-Aminoethylamino)propyl]trimethoxysilane (AEAPTMS). The synthesized nanoparticles were characterized by TGA, N₂ adsorption, SEM, FTIR, CHN elemental analysis. The total weight loss for the modified SBA-15 is 15.2% and thermal analysis revealed that 1.5 mmol AEAPTMS/1g SBA-15 had been grafted. The modified particles were used as a drug delivery system. Ibuprofen as common nonsteroidal anti-inflammatory drug was used to evaluate the controlled drug release properties of modified SBA-15. The results show that the modification of SBA-15 with organic groups such as [3-(2-Aminoethylamino)propyl] trimethoxysilane and (3-aminopropyl)triethoxysilane (APTES) improve the organophilicity of the SBA-15 and the drug loading efficiency. The results of drug delivery experiments reveal that the surface modification of SBA-15 with amino groups significantly decreases the drug delivery rate. The data obtained from the in vitro release studies was used to evaluate the kinetic mechanism of release; the initial 60% release of drug at pH 7.4 fits with the Korsmeyer–Peppas model, when diffusion is the main drug release mechanism.

Keywords: Drug delivery, Ibuprofen, Nano silica, SBA-15, Surface Modification.

1. INTRODUCTION

Controlled release technologies are more important in modern medication and pharmaceuticals. Controlled drug release at a desired rate has numerous advantages over common forms of dosage such as maintaining the patient's blood drug level, minimizing harmful side effects, prolonging productivity time, heightening

bioavailability and improving patient compliance [1].

Mesoporous silica based materials are currently a field of intensive active research because of their high potential in a very broad range of applications [2] such as catalytic supports in fine chemistry [3], pharmaceutical industry [4], as well as for

the production of special polymer materials [5]. Large surface areas, ordered mesoporous structure, tunable pore sizes and volumes and well-defined surface properties for chemical modification are the attractive features of the mesoporous silica materials that make them as one of the most important drug carrier materials for controlled drug delivery [6].

Porous silica materials can be easily modified by various functional groups. As a member of mesoporous silica materials, SBA-15 materials were widely studied due to its excellent chemical and thermal stability [7, 8] and ease of chemical modification that makes it a good candidate to be used as a drug delivery system of drugs such as ibuprofen [9, 10]. Three methods are used to modify the surface of mesoporous silica materials including: co-condensation (one-pot synthesis), grafting (post-synthesis modification) and imprint coating method [11, 12]. Various functional groups are introduced onto silica surface including amino alkyl [13, 14], cyano alkyl [15, 16], epoxy alkyl [17], metal-amino alkyl [12], etc. Various functionalized SBA-15 materials and model drugs can form the host-guest interaction between the drug and silica formed via different molecular interactions such as ionic bond reaction and hydrogen bonding effect [14]. These surface interactions prolong the drug release to tackle the problem of drug leakage in the release procedure, while excellently solve the issue of site-selectivity.

Even it has been previously shown that MCM-41 can be used for controlled release of ibuprofen under in vitro conditions [18-21], SBA-15 is a superior drug carrier due to its higher chemical and thermal stability of SBA-15 [22,23]. However, other mesoporous materials has been investigated to gain control over the releasing pattern of the guest drug [24-26]. Functionalization of SBA-15 using [3-(2-Aminoethylamino)propyl]trimethoxysilane (AEAPTMS) and its application as a

carrier for drug delivery system has not yet been reported. In this study, ibuprofen was selected as a model drug for evaluating the loading and release capability of the prepared modified SBA-15. Ibuprofen is a well-known non-steroidal anti-inflammatory drug and has been widely used for the treatment of inflammation, pain and rheumatism. But this drug has a short biological half-life (2 h) [27], which makes the prepared modified SBA-15 a suitable candidate for sustained or controlled drug delivery of ibuprofen. Modification of SBA-15 was done by AEAPTMS and compared with SBA-15 modified by (3-aminopropyl)triethoxysilane [28]. Functionalized SBA-15 was applied as a carrier for adsorption of Ibuprofen. In vitro release behavior of the modified SBA-25 was also studied.

2. EXPERIMENTAL

2.1. Materials

Poly (ethylene oxide)-block-poly (propylene oxide)-block-poly (ethylene oxide) [Pluronic P123, [(EO)₂₀(PO)₇₀(EO)₂₀] was obtained from Aldrich. Tetraethyl orthosilicate (TEOS) and [3-(2-Aminoethylamino) propyl] trimethoxysilane (AEAPTMS), toluene, n-hexane, ethanol and dichloromethane were purchased from Merck. Ibuprofen (IBU) was purchased from Darupakhsh Company with 99.9% purity. Toluene and n-hexane were refluxed over sodium with benzophenone as an indicator and distilled under nitrogen atmosphere before use. Dichloromethane was dried by distilling over P₂O₅ under nitrogen atmosphere.

2.2. Instrument and equipment

UV-Vis spectroscopy measurements were done by Shimadzu UV-1650PC UV-visible spectrophotometer. The FT-IR spectra of the samples were recorded by FT-IR (Perkin-Elmer, 580 B) in the range between 400 and 4000 cm⁻¹ at room

temperature from KBr pellets. The morphologies were recorded using a Scanning Electron Microscope (Cambridge S-360). The thermo gravimetric measurements were performed by SDT 2960 instrument with a heating rate of 10°C/min in air flow. Carbon, hydrogen and nitrogen contents of the samples were determined using a Vario EL III CHN elemental analyzer. Nitrogen adsorption–desorption isotherms were obtained at 77 K using an OMNISORP (TM) 100CX VER 1G adsorption apparatus. Samples were outgassed at 473 K for at least 8 h in vacuum prior to measurements.

2.3. Synthesis of SBA-15

SBA-15 material was prepared according to the procedure reported by Zhao et al. [8] using Pluronic 123 as a structure-directing agent and TEOS as a silica source. First, 4.0 g of Pluronic P123 was dissolved in 30 g of water and 120 g of 2 M HCl solution at 35 °C. Then 8.5 g of TEOS was added into the solution at 35 °C and stirred for 20 h. After all, the mixture was aged at 80 °C overnight under static condition. The solid product was filtered off, washed and air-dried at room temperature. The as-synthesized sample is denoted as SBA-15(SY). The template was removed from the as-made SBA-15 by Soxhlet extraction with ethanol for 72 hours followed by calcination at 550 °C for 6 h (SBA-15). Synthesis procedure is shown in Figure 1.

2.4. Modification of SBA-15 by [3-(2-Aminoethylamino)propyl] trimethoxysilane

Modification of the SBA-15 with amino groups was according to our previous work [28]. In a typical method, 3.0 g of silica was placed in a 100 mL round bottom flask with 50 mL of dry toluene and 2.4 g of AEAPTMS (48 h, 110 °C) in toluene. Then the mixture was refluxed at 110 °C for 48 h under the protection of nitrogen. After 48 h the product was washed with toluene, n-hexane and dichloromethane respectively and dried at 25°C for 12 h. This material is denoted as SBA-15-NH-NH₂. Surface modification of the sample is shown schematically in Figure. 2.

2.5. Drug loading and release

The loading of the drug was carried out by the immersion of silica samples at 40 °C with n-hexane solution containing 30 mg/cm³ of ibuprofen for 35h under stirring rate of 100 rpm.

In our previous work [28], different drug to SBA-15 ratios were selected to find the optimum amount of drug used for loading. The highest drug loading efficiency, that is, 50% was achieved using a drug loading of Ibuprofen/SBA-15 ratio of 50:100 (w/w). Finally, ibuprofen loaded samples were centrifuged (750 rpm, 5 min); the residue was washed with n-hexane and dried for 3 h at 80 °C in oven. The drug loading (DL%) efficiency was calculated by the equation (1):

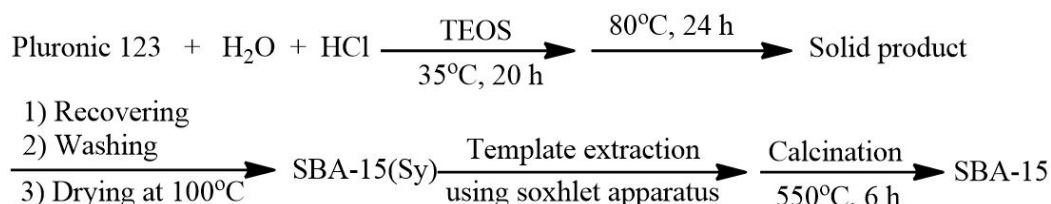


Figure 1. Procedure of SBA-15 synthesis

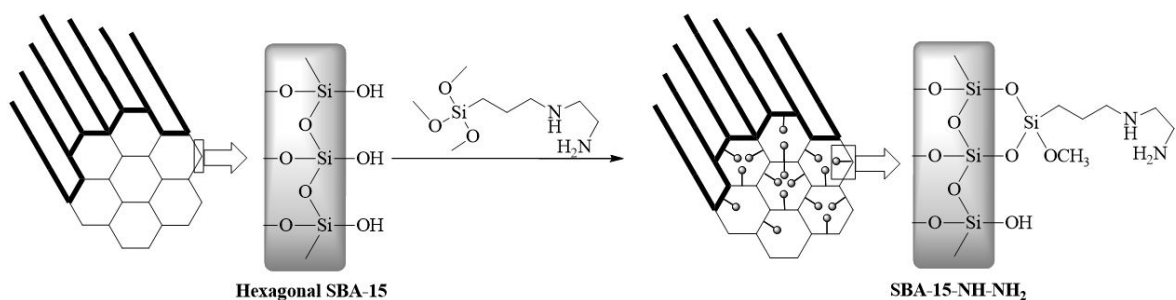


Figure2. Schematic of amine functionalization of SBA-15

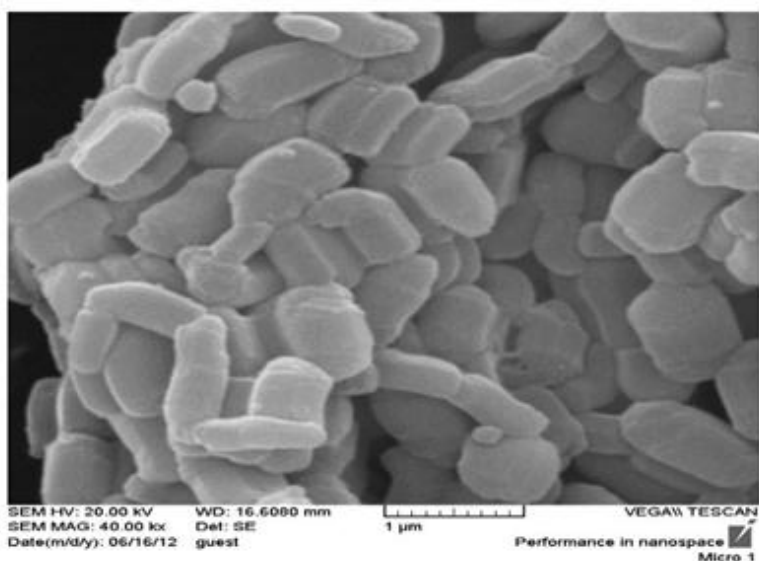


Figure3. SEM image of SBA-15

m_1 is the initial weight of drug before loading, m_2 is the weight of the drug in the solution after loading achieved by measuring UV-Vis absorbance at 224 nm, m_3 is the initial weight of SBA-15 [29].

$$DL\% = \frac{m_1 - m_2}{m_3} * 100 \quad (1)$$

To study the *in vitro* release of ibuprofen from SBA-15, the loaded powder was immersed into simulated body fluid (SBF) with pH=7.2-7.4, under magnetic stirring in an interpenetrating membrane. At predetermined time intervals, 2 mL samples were withdrawn and immediately replaced with an equal volume of dissolution medium to keep the volume constant. These samples were properly diluted and analyzed for ibuprofen content at 224 nm using UV-Vis

spectrophotometer. All the experiments were performed in triplicate. The concentration of the released drug at each interval is evaluated by equation (2). The Cumulative release (CR%) of ibuprofen is evaluated by equation (3);

$$C_n = C_N + \frac{C_{n-1}V_1}{V_t} \quad (2)$$

$$CR\% = \frac{C_n * V_t}{m_1 - m_2} * 100 \quad (3)$$

C_n , C_N , V_1 and V_t are the actual concentration of ibuprofen, the apparent concentration of ibuprofen, the volume of the sample taken at each time and the total volume of the release medium, respectively.

3. RESULTS AND DISCUSSION

3.1. Material characterization

SEM images reveal that the SBA-15 consists of many rope-like domains with relatively uniform sizes of $\sim 1 \mu\text{m}$ (Figure. 3), as demonstrated by the other researchers [7-8, 26]

Figure 4 shows nitrogen adsorption-desorption isotherm plot from the adsorption branch of hexagonal SBA-15 [7, 8]. P/P_0 is surface pressure to preliminary pressure ratio. It can be observed that the nitrogen adsorption/desorption isotherms of the SBA-15 were typical type IV isotherms according to the IUPAC classification. Table 1 summarizes the textural properties of the SBA-15 supports derived from nitrogen adsorption-desorption isotherm plot and pore size distribution curve.

Figure.5 shows the FTIR spectra of the SBA-15(SY), calcined SBA-15 and SBA-

15-NH-NH₂ carriers before ibuprofen adsorption. For all samples, the asymmetric stretching vibrations of Si-O-Si bands around 1070-1220 cm^{-1} associated with the formation of a condensed silica network are present [26]. The peak at 3400 cm^{-1} is attributed to the O-H stretching vibration mode. For uncalcined sample, the peaks at 2850-3000 cm^{-1} and 1465 cm^{-1} are caused by the C-H stretching and CH₂ bending of Pluronic 213, respectively, which are not significantly observed for the calcined sample.

SBA-15 sample modified by AEAPTMS shows the bands at 2916 and 1540 cm^{-1} , which are attributed to C-H and N-H stretching vibrations of (Aminoethylamino)propyl anchored on the surface of mesoporous support. These characteristic bands confirm that [3-(2-Aminoethylamino)propyl] groups of AEAPTMS were introduced into SBA-15 [30, 31].

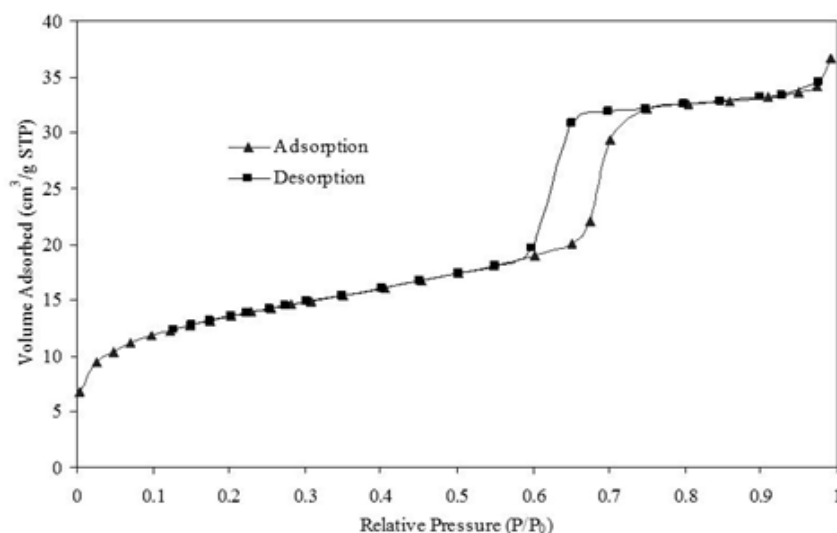


Figure 4. Nitrogen adsorption-desorption isotherm plot of SBA-15.

Table 1. Structural parameters of SBA-15

Code	S_{BET} (m^2/g)	d_p (Å°)	V_p (ml/g)	d_{100} (Å°)	b_p (Å°)
SBA-15	479	35.8	0.51	87	32.4

S_{BET} , BET specific surface area; V_p , specific pore volume; d_p , average pore diameter, obtained from BJH adsorption data, $d_p = 4V_p/S_{\text{BET}}$; d_{100} , XRD interplanar spacing; b_p , pore wall thickness, $b_p = (a_0 - d_p)/2$, $a_0 = (2/\sqrt{3})d_{100}$.

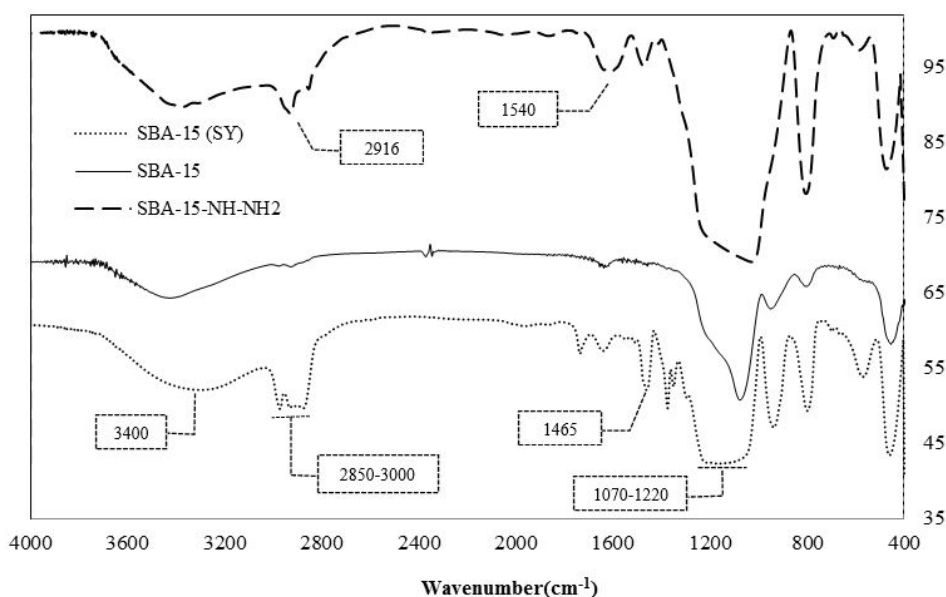


Figure 5. FTIR spectra of SBA-15 before calcination (SBA-15 (Sy)) and after calcination (SBA-15), SBA-15-NH-NH₂

TGA analysis was done to confirm the AEAPTMS grafting on SBA-15 (Figure. 6). The weight loss for all samples occurred in the temperature between 250 °C and 700 °C [26, 28]. The rate of weight loss illustrates the gradual removal of organic groups of the SBA-15. TGA curve of SBA-15(Sy) shows total weight loss of 54 wt % (Figure. 6A). The TGA curve of SBA-15 after calcination indicates that the most of the organic materials were removed. So the weight loss is attributed to removal of template and adsorbed water molecules.

[3-(2-Aminoethylamino)propyl] content of SBA-15-NH-NH₂ was determined by the weight loss measurement of the sample from Figure. 6B. As shown in Figure. 6B maximum weight loss has been occurred in the range of 200-700 °C which is related to the gradual removal of the aliphatic groups as shown by Wang et al. [26]. The sample has three weight loss steps at this range. The first loss occurs near 256 °C for terminal amine groups (NH₂) and the second one is at ~330 °C for second amine groups (NH) and the third one happens at ~603 °C for aliphatic groups (ethyl and propyl groups). The total weight loss for the SBA-15-NH-NH₂ is 15.2%.

Furthermore, thermal analysis revealed that 1.5 mmol AEAPTMS/1g SBA-15 had been grafted [28].

CHN elemental analysis was applied for determination of carbon, hydrogen and nitrogen contents of the samples, (Table 2). In comparison to unmodified SBA-15, the results show significant increase in carbon, nitrogen and hydrogen contents of SBA-15-NH-NH₂, which is in good accordance with TGA/DTA and approves the grafting of 3-(2-aminoethylamino)propyl groups on SBA-15.

3.2. Drug loading efficiency

In order to obtain the effect of modifying procedures on drug loading, we calculate the DL% for unmodified and modified SBA-15. The results are shown in table 3. As shown in table 3, modification procedure enhanced the drug loading percentage. So the results show that in the presence of organic groups such as [3-(2-Aminoethylamino)propyl]trimethoxysilane (AEAPTMS) and (3-aminopropyl)triethoxysilane (APTES), the organophilicity of the SBA-15 can improve the drug loading [32]. Ibuprofen probably adsorbs to the amine

functionalized SBA-15 surface by hydrogen bonds between NH and NH₂ groups of amine groups and COOH groups of ibuprofen (Figure. 7). Comparing the DL of the SBA-15 modified by 3-aminopropyltriethoxysilane (SBA-15-

NH₂) and SBA-NH-NH₂ reveals that there is not a significant difference between the influence of amine groups of APTES and AEAPTMS on loading efficiency of the modified SBA-15.

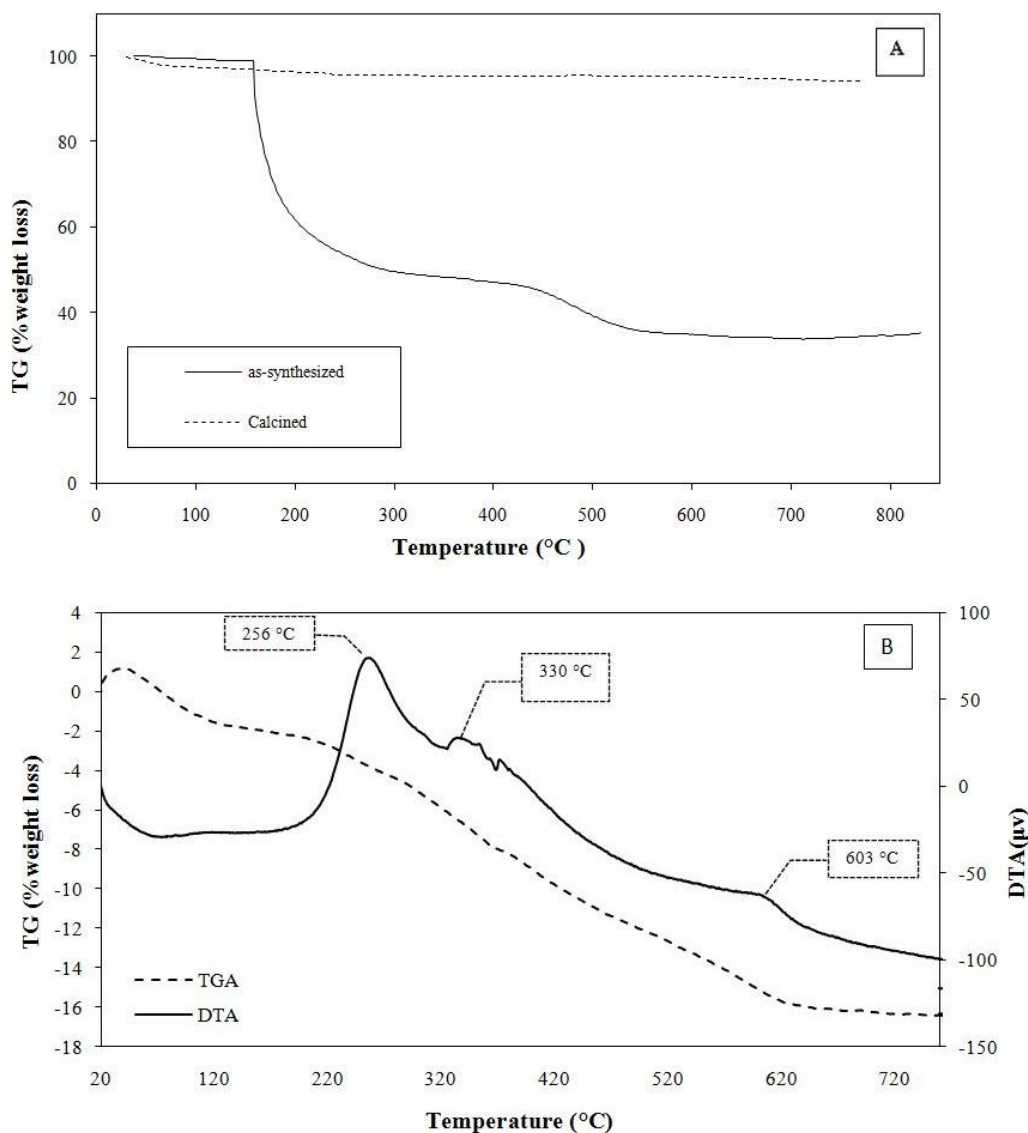


Figure 6. TGA curves of as synthesized and calcined SBA-15 (A). DTA and TGA analysis of SBA-15-NH-NH₂ (B)

Table 2. Elemental analysis of the SBA-15 and SBA-15-NH-NH₂

Element content	C (wt %)	H (wt %)	N (wt %)
SBA-15	12.1	2.9	<0.1
SBA-15-NH-NH ₂	24.89	5.81	7.29

Table 3. Drug loading of different type of SBA-15

Sample	SBA-15	SBA-15-NH ₂	SBA-15-NH-NH ₂
DL%	40±2	51±2	49±2

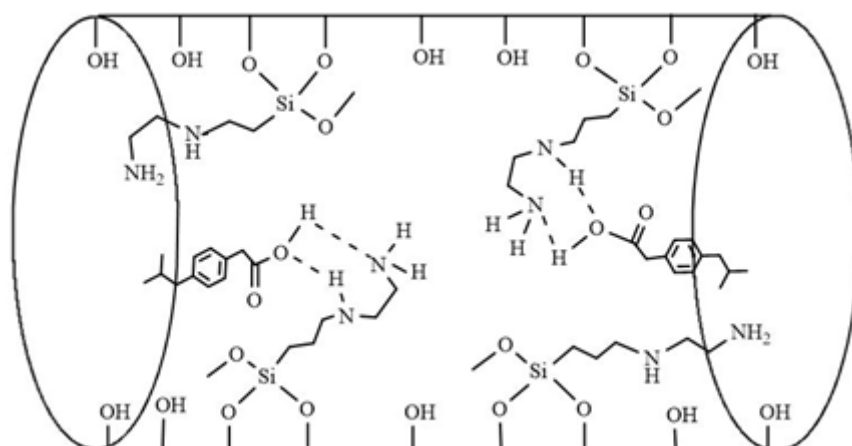


Figure 7. Interaction of Ibuprofen with SBA-15-NH-NH₂

3.3. Drug delivery

The drug release profiles of samples in SBF are depicted in Figure. 8. Release of ibuprofen from mesoporous materials reaches the maximum amount (100 percent) after 300 hour. Hydrogen bonding between ibuprofen and the parent mesoporous silica materials is relatively weak, so the mass transfer of ibuprofen molecules through the channels is controlled by diffusion [6].

Figure 8 displays the cumulative release of ibuprofen from SBA-15, SBA-15-NH₂ and SBA-15-NH-NH₂. From Figure 8A, for SBA-15, after 8 h, 60% of the drug can release and 40% of it traps in the mesoporous structure. Additionally, for pure SBA-15, burst release of ibuprofen occurs and after 2 h the amount of released IBU becomes constant. It means that, this material cannot gradually release the drug and it is not an appropriate carrier for sustained drug delivery.

So the SBA-15 was modified by amine groups of AEAPTMS and APTES. Effect of amino-functionalization has been studied by comparing the drug delivery profile of pure SBA-15 and amine-modified SBA-15 materials. Figures. 8A and 8B show the cumulative release (CR) % of ibuprofen from SBA-15-NH-NH₂ and SBA-15-NH₂. The release behavior of the SBA-15-NH-NH₂ is similar to SBA-15-NH₂ with a little change in release rate and

release time [29]. It is obvious that by functionalization of the SBA-15 compared with SBA-15, the burst release did not occur and it took a long time for the ibuprofen to release from SBA-15-NH-NH₂ and SBA-15-NH₂. This phenomenon is related to the hydrogen bonding between the carboxylic groups of ibuprofen and amine groups of modified SBA-15 that is stronger than the interaction between silanol groups of the parent silica and ibuprofen. This can explain the slower release rates of ibuprofen from SBA-15-NH-NH₂ samples in comparison with SBA-15.

By comparing the results of Figure 8A and B, it can be concluded that using the modified SBA-15 in place of pure SBA-15, the drug delivery has occurred in a longer period of time. Using SBA-15-NH₂, drug delivery happened over 225 h with a relatively constant rate, while it takes 300 h for SBA-15-NH-NH₂. The two amine groups with their steric hindrance on the surface of silica not only slightly decrease the drug loading efficiency but also increase the time of release.

In order to analyze the data obtained from the in vitro release studies and to evaluate the kinetic release mechanism, the initial 60% data related to the release of drug at pH 7.4 was fitted with the Korsmeyer–Peppas model - a simple, semi-empiric model, when diffusion is the main drug release mechanism.

$$\frac{M_t}{M_\infty} = kt^n$$

Where M_t/M_∞ is a fraction of drug released at time t , k is a kinetic constant characterizing the drug-carrier system, while n is an exponent that characterizes the mechanism of drug release. If the exponent $n \leq 0.45$, then the drug release mechanism is a Fickian diffusion, if $0.45 < n < 0.89$, then it is a non-Fickian or anomalous diffusion, $n = 0.89$ to Case II (relaxational) transport and $n > 0.89$ to

super case II transport [33, 34]. For systems exhibiting Case II transport, the dominant mechanism for drug transport is due to polymer relaxation as the gels swells. These types of devices, known as swelling-controlled release systems.

According to Table 4, the drug was released by a super case II transport and non-Fickian diffusion mechanism from SBA-15 and SBA-15-NH-NH₂, respectively.

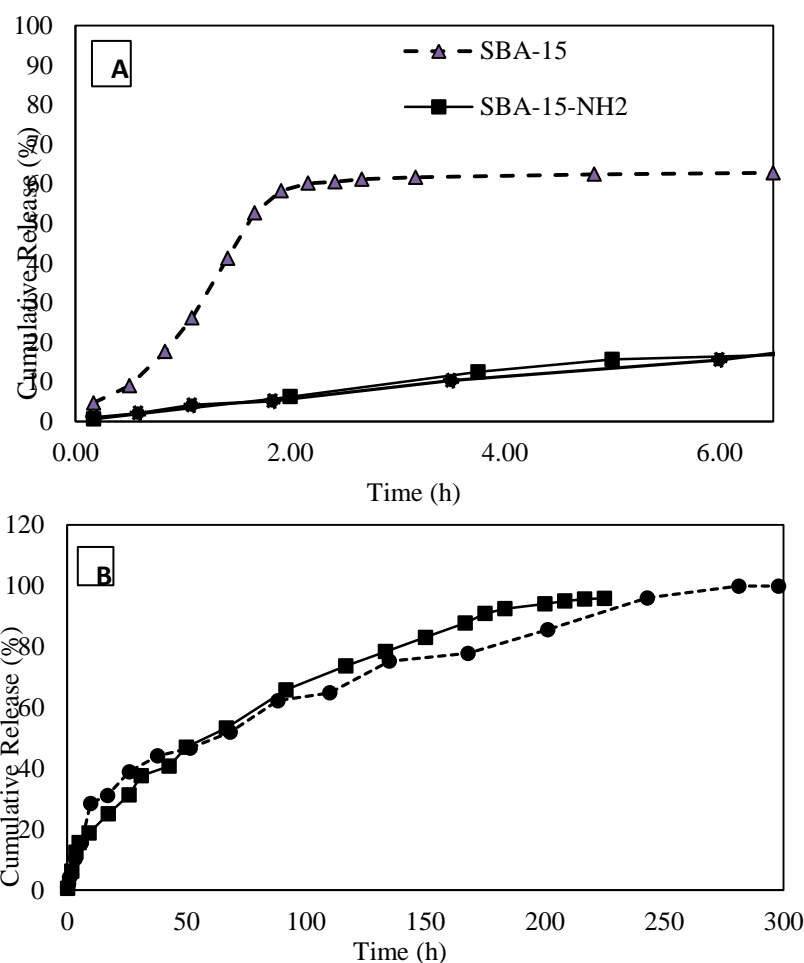


Figure 8. Cumulative release (CR) % of Ibuprofen from (A) SBA-15, SBA-15-NH₂ and SBA-15-NH-NH₂ after 8h, (B) SBA-15-NH₂ and SBA-15-NH-NH₂ after 300 h.

Table 4. Ibuprofen release kinetic parameters for silica materials in PBS (Korsmeyer-Peppas model)

Model		R ²	n	k	Mechanism
Korsmeyer-Peppas	SBA-15	0.9671	1.0746	0.0031	super case II transport
	SBA-15-NH-NH ₂	0.9678	0.7232	0.0019	non-Fickian

4. CONCLUSION

Mesoporous SBA-15 has been synthesized and functionalized by AEAPTMS successfully. Adsorption of ibuprofen occurs with much better yields (49%) on the modified surface. Comparing the release profiles showed that surface functionalization of mesoporous silica with amine groups leads to controlled release of ibuprofen without burst release at initial times. Also, by functionalization of SBA-15 with amino groups the release rate becomes slower. Furthermore, loading and release medium conditions have significant effects on drug delivery rates.

REFERENCES

1. K. E. Uhrich, S. M. Cannizzaro, R. S. Langer and K. M. Shakesheff: *Chem. Rev.*, Vol. 99, (1999), pp. 3181-3198.
2. C. T. Kresge, M. E. Leonowicz, W. J. Roth, J. C. Vartuli and J. S. Beck: *Nature*, Vol. 359, (1992), pp. 710-712.
3. A. Corma: *Chem. Rev.*, Vol. 97, (1997), pp. 2373-2419.
4. T. P. Corine, D. Brunel, S. Begu, B. Chiche, F. Fajula, D. A. Lerner and J. M. Devoisselle: *New J. Chem.*, Vol. 27, (2003), pp. 1415-1418.
5. T. P. Corine, D. A. Lerner, C. Charnay, L. Nicole, S. Begu and J. M. Devoisselle: *Chem. Phys. Chem.*, Vol. 4, (2003), pp. 281-286.
6. A. Szegedi, M. Popova, I. Goshev and J. Mihaľy: *Sol. State Chem.*, Vol. 184, 2011, pp. 1201-1207.
7. D. Y. Zhao, J. L. Feng, Q. S. Huo, N. Melosh, G. H. Fredrickson, B. F. Chmelka and G. D. Stucky: *Science*, Vol. 279, (1998), pp. 548-552.
8. D. Y. Zhao, Q. S. Huo, J. L. Feng, B. F. Chmelka and G. D. Stucky: *J. Am. Chem. Soc.* Vol. 120, (1998), pp. 6024-6036.
9. Y. J. Yang, X. Tao, Q. Hou and J. F. Chen: *Acta Biomater.* Vol. 5, (2009), pp. 3488-3496.
10. W. Xu, Q. Gao, Y. Xu, D. Wu, Y. Sun, W. Shen and F. Deng: *Powder Technol.*, Vol. 191, (2009), pp. 13-20.
11. S. Zhu, Z. Zhou, D. Zhang, C. Jin, Z. Li, *Micropor. Mesopor. Mat.* 106 (2007) 56-61.
12. M. C. Burleigh, S. Dai, E. W. Hagaman, C. E. Barnes and Z. L. Xue: *ACS Symp. Series*, Vol. 778, (2001), pp. 146-158.
13. I. I. Slowing, J. L. Vivero-Escoto, C. W. Wu and V. S. Y. Lin: *Adv. Drug Deliv. Rev.*, Vol. 60, (2008), pp. 1278-1288.
14. D. R. Radu, C. Y. Lai, J. Huang, X. Shu and V. S. Y. Lin: *Chem. Commun.* Vol. 10, (2005), pp. 1264-1266.
15. S. Huh, H-T. Chen, J. W. Wiench, M. Pruski and V. S. Y. Lin: *Angew. Chem. Int. Ed.*, Vol. 44, (2005), pp. 1826-1830.
16. S. Huh, J. W. Wiench, J. C. Yoo, M. Pruski, and V. S. Y. Lin: *Chem. Mater.*, Vol. 15, (2003), pp. 4247-4256.
17. D. R. Radu, C-Y Lai, J. W. Wiench, M. Pruski, V. S. Y. Lin: *Am. Chem. Soc.*, Vol. 126, (2004), pp. 1640-1641.
18. C. Charnay, S. Bégu, C. Tourné-Péteilh, L. Nicole, D. A. Lerner and J. M. Devoisselle: *Eur. J. Pharm. Biopharm.*, Vol. 57, (2004), pp. 533-540.
19. M. Vallet-Regí, A. Ramila, P. R. del Real and J. Perez-Pariente: *Chem. Mater.*, Vol. 13, (2001), pp. 308-311.
20. A. Ramila, B. Munoz, JPPariente and MR Vallet: *J. Sol-Gel Sci. Technol.*, Vol. 26, (2003), pp. 1199-1202.
21. P. Horcajada, A. Ramila, P. Z. Perez and R. M. Vallet: *Micropor. Mesopor. Mater.*, Vol. 68, (2004), pp. 105-109.
22. A. L. Doadrio, E. M. B. Sousa, J. C. Doadrio, J. P. Pariente, B. I. Izquierdo and R. M. Vallet: *J Control Release* Vol. 97, (2004), pp. 125-132.

23. R. M. Vallet, J. C. Doadrio, A. L. Doadrio, B. I. Izquierdo and J. P. Pariente: *Solid State Ionics*. Vol. 172, (2004), pp. 435-439.
24. H. J. Kim, J. E. Ahn, S. J. Haam, Y. G. Shul, S. Y. Song and T. S. Tatsumi: *J. Mater. Chem.*, Vol. 16, (2006), pp. 1617-1621.
25. J. C. Doadrio, E. M. B. Sousa, I. B. Isabel, A. L. Doadrio, P. J. Pariente and R. M. Vallet: *J. Mater. Chem.*, Vol. 16, (2006), pp. 462-466.
26. H. Wang, X. Gao, Y. Wang, J. Wang, X. Niu and X. Deng: *Ceram. Int.* Vol. 38, (2012), pp. 6931–6935.
27. K. D. Rainsford: (1999). "Ibuprofen: A Critical Bibliographic Review" London, Taylor & Francis., pp. 53-86.
28. E. Ahmadi, N. Dehghannejad, S. Hashemikia, M. Ghasemnejad and H. Tabebordbar: *Drug Deliv.*, Vol. 21, (2014), pp. 164-72.
29. S. Hashemikia, N. Hemmatinejad, E. Ahmadi, M. Montazer, *Journal of colloid and interface science* 443, (2015), pp. 105-114.
30. H. Wang, X. Gao, Y. Wang, J. Wang, X. Niu and X. Deng: *Ceram. Int.*, Vol. 38, (2012), pp. 6931–6935.
31. Y. Xu, C. Wang, G. Zhou, Y. Wu and J. Chen: *Appl. Surf. Sci.*, Vol. 258, (2012), pp. 6366– 6372.
32. S.W. Song, K. Hidajat and S. Kawi: *Langmuir*, Vol. 21, (2001), pp. 9568-9575.
33. P. L. Riger and N. A. Peppas: *J. Control. Rel.* Vol. 5. (1987), pp. 37-42.
34. J. Siepmann and N. A. Peppas: *Adv. Drug Deliv. Rev.*, Vol. 48, (2001), pp. 139-157.